Journal of Thermal Analysis and Calorimetry, Vol. 61 (2000) 75–89

HEAT CAPACITY MEASUREMENTS USING TEMPERATURE-MODULATED HEAT FLUX DSC WITH CLOSE CONTROL OF THE HEATER TEMPERATURE

R. Androsch

Institute of Material Science, Martin Luther University Halle–Wittenberg, Geusaer Str. 06217 Merseburg, Germany

(Received January 11, 2000)

Abstract

The determination of heat capacity data with sawtooth-type, temperature-modulated differential scanning calorimetry is analyzed using the Mettler-Toledo 820 ADSC™ temperature-modulated differential scanning calorimeter (TMDSC). Heat capacities were calculated via the amplitudes of the first and higher harmonics of the Fourier series of the heat flow and heating rates. At modulation periods lower than about 150 s, the heat capacity deviates increasingly to smaller values and requires a calibration as function of frequency. An earlier derived correction function which was applied to the sample temperature-controlled power compensation calorimeter enables an empirical correction down to modulation periods of about 20 s. The correction function is determined by analysis of the higher harmonics of the Fourier transform from a single measurement of sufficient long modulation period. The correction function reveals that the time constant of the instrument is about 5 s rad^{-1} when a standard aluminum pan is used. The influence of pan type and sample mass on the time constant is determined, the correction for the asymmetry of the system is described, and the effect of smoothing of the modulated heat flow rate data is discussed.

Keywords: DSC, Fourier transformation, heat capacity, sawtooth-modulation, TMDSC

Introduction

Temperature-modulated differential scanning calorimetry, TMDSC, [1] has the potential to increase the precision in the experimental evaluation of the heat capacity of materials [2] since it permits to exclude the more or less random heat losses common in any type of calorimetry from a signal that is modulated with a fixed frequency [3]. Another striking advantage, compared to standard differential scanning calorimetry, DSC, is the opportunity to determine the heat capacity in presence of irreversible effects [1], and with quasi-isothermal experiments [3, 4], i.e., experiments where the temperature is modulated about a constant base temperature, T_o.

In transition regions, a DSC cannot separate the total heat flow rate, $HF=\mathrm{d}Q/\mathrm{d}t$ (where Q is the heat exchanged) into its two components which are caused by the la-

1418–2874/2000/ $ 5.00

Akadémiai Kiadó, Budapest
Kluwer Academic Publishers, Dordrecht

tent heat, L, which on absorption or evolution by a sample does not change its temperature, and the thermodynamic heat capacity, $C_p=(\partial Q/\partial T)_{p,n}$, where the subscript indicates that the experiment is carried out at constant pressure and unchanged composition. Furthermore, the determination of C_p by DSC requires a rather broad temperature interval for analysis since $HF(t)$, in form of the asymmetry-corrected and energy-calibrated value, can only be determined after steady state has been reached [2]:

$$C_p^{\text{standard DSC}} \approx \frac{HF(t)}{q} \tag{1}$$

where q (= dT_s/dt) is the constant heating rate of the sample. Depending on q, the Newton's law constant of the calorimeter, and the heat capacity of the sample, at least 5 to 10 K need to be scanned before steady state is reached and measurement can begin. In TMDSC, in contrast, the approach to steady state does not have to be awaited for analysis which considerably shortens the time to begin a heat capacity determination. Typical modulation amplitudes of the sample temperature, A_{Ts}, are between 0.1 and 2 K. The sample may be probed by an underlying heating rate, $<q>$, which represents the average q over one modulation period p, and a periodic sample temperature oscillation, which in most cases is sinusoidal or sawtooth-like with frequency $\omega=2\pi/p$ with p typically chosen between 10 and 200 s.

The calorimetric response in form of a modulated heat flow rate is deconvoluted into its different components by a Fourier transformation. The 0th Fourier coefficient is the average over one modulation cycle, $<HF(t)>$, and is called the total heat flow rate and represents in many cases a result similar to the heat flow rate of the standard DSC. Using a sinusoidal modulation, the amplitude of the first harmonic is called the reversing component, A_{HF}. In this case, differences between the total and reversing component define the non-reversing heat flow rate [1, 4]. For non-sinusoidal modulation or calorimeter response higher harmonics of the Fourier series are needed for a detailed description of $T_s(t)$ and $HF(t)$ in addition to the first harmonic. Specifically when the temperature-modulation is in form of a centrosymmetric sawtooth, the Fourier series becomes:

$$HF(t)-<HF(t)>=\frac{8A_{HF}}{\pi^2}\sum_{\nu=1,3,5,7,\ldots}\left[\frac{-1^{\frac{\nu+3}{2}}}{\nu^2}\sin(\nu\omega t)\right] \tag{2}$$

where ν is the order of the harmonics.

Both, $<HF(t)>$ and the Fourier components of the heat flow rate can be used to calculate an apparent heat capacity, $C_p^{\#}$, i.e., a heat capacity that may contain additional contributions to the reversible, thermodynamic heat capacity:

$$C_p^{\#\,\text{total}} \approx \frac{<HF(t)>}{<q>} \tag{3}$$

and

$$C_p^{\#\,rev} = \frac{A_{HF}(\nu\omega)}{\nu\omega A_{TS}(\nu\omega)} K(\nu\omega) \tag{4}$$

where $A(\nu\varpi)$ stands for the amplitudes of the reversing quantities obtained from the appropriate Fourier coefficients of frequency $\nu\omega$, and $K(\nu\omega)$ is a constant which will to be discussed below. For sinusoidal modulation only the first harmonic is nonzero. For sawtooth modulation the higher harmonics can also be analyzed [5] as suggested by Eq. (2). Note that according to the definition of $q(t)$, the corresponding amplitude $A_q(\nu\omega)=\nu\omega\, A_{Ts}(\nu\omega)$.

The heat capacity calculated from Eq. (3) contains, as in standard DSC, Eq. (1), all heat capacity contributions, latent heat effects, and random heat losses. The heat capacity calculated from Eq. (4) contains only reversing contributions. In the absence of irreversible latent heats and random heat losses Eqs (3) and (4) give identical results which, however, may still only be apparent heat capacities, $C_p^{\#}$, rather than the true thermodynamic C_p. Reversing latent heats would contribute to Eq. (4), but may be identified by their slower kinetics. Similarly, in the glass transition region a part of the heat capacity itself becomes time dependent due to the freezing of the cooperative, conformational contributions at lower temperature [6]. In both of these cases a frequency-dependent measurement is of unique value to separate the frequency-independent heat capacity and to study the kinetics of the other contributions.

Quasi-isothermally performed TMDSC experiments which are characterized by $\langle q\rangle=0$ are of particular value for thermal analyses. In the absence of latent heats, the total heat flow rate $\langle HF(t)\rangle=0$ should be zero. Any positive or negative result from Eq. (3) indicates a slow sample response that can be assessed quantitative. Since quasi-isothermal experiments have no time limit other then the patience of the operator, wide ranges of kinetic studies can be undertaken. Furthermore, details of the kinetics can be extracted by an analysis of the heating and cooling cycles in the time domain.

Initially, the correction function $K(\nu\varpi)$ was developed for a sinusoidally modulated heat flux calorimeter ($\nu=1$) operating under steady state conditions, with the same Newton's law constant K' for sample and reference calorimeters, and a heat capacity of the reference calorimeter of C_R [4]:

$$K(\omega)=\sqrt{\left(\frac{K'}{\omega}\right)^2 + C_R^2} = \sqrt{1+\tau^2\omega^2} \tag{5}$$

The second part of Eq. (5) generalizes this equation, so that it also applies empirically to other calorimeters than for the TA Instruments, MDSC™ , when steady state is not maintained. In these cases, $K(\omega)$ can be determined by measurements at different frequencies ω, or by using sawtooth modulation and analyzing higher harmonics (ω becomes then $\nu\omega$). Plotting the inverse of the squared, uncorrected heat capacity as obtained by Eq. (4) with $K(\nu\omega)=1$ *vs*. the square of the frequency reveals τ and the correct value of the heat capacity [7]:

$$\left(\frac{1}{C_p^{\text{uncorr.}}}\right)^2 = \left(\frac{1}{C_p^{\text{corr.}}}\right)^2 [1+\tau^2\nu^2\omega^2] \tag{6}$$

Initially, τ was determined for a power-compensated, sawtooth-modulated TMDSC from the first harmonic of the Fourier series from measurements at different frequencies ω [7]. Later, it was shown that the higher harmonics of the Fourier transform at frequencies $\nu\omega$ can also be used to determine the correction function [5].

Equation (5) was derived assuming the same Newton's-law constant for reference and sample calorimeters and steady state which is not dependent on sample properties like mass and heat transfer conditions. When applying Eq. (5) to the power-compensating calorimeter of Perkin Elmer, a strong dependence of τ on sample properties was found [7]. The explanation lies in the importance of the heat transfer into and throughout the sample since the overall path from the heater is relatively short compared to heat flux instruments [8]. The smaller the time constant of the instrument, the larger is the influence of sample properties on the overall time constant τ. The time constant of a particular experiment contains an instrumental part, τ_{inst}, and a sample part, τ_{sample}:

$$\tau = \tau_{\text{inst}} + \tau_{\text{sample}} \tag{7}$$

If the instrumental contribution is rather small, as in the power-compensation calorimeter, the sample part will be dominant, in contrast to the heat flux calorimeter with control at the sample position, where τ_{inst} is dominant. Furthermore, one expects that τ is independent on frequency as long as the temperature gradient within the sample is negligible, and τ increases with ω as the temperature gradient becomes significant.

In the present paper an effort is made to test the performance of a heat flux calorimeter where the control of the modulation is close to the heater using quasi-isothermal heat capacity measurements in terms of Eqs (4) to (6). A calorimeter that fits this condition is the Mettler-Toledo DSC 820. It was shown before that modeling of this calorimeter was complicated, particularly for the standard operation with reference and sample pans [9]. In the present analysis we attempt to empirically determine the time constant τ and the influence of typical experimental parameters on the reproducibility of the correction function $K(\nu\omega)$. We used a sawtooth-modulation for the program temperature, for reason of compatibility with earlier investigations [5, 7] and the inability of the chosen instrument to realize a symmetric sinusoidal oscillation [9].

The Mettler-Toledo STAR^e Software does not support the heat capacity calculation via the Fourier transform in sawtooth-modulated experiments. The calculation of the heat capacity from sawtooth-modulation experiments using the instrument software requires steady state before switching the heating rate of the sawtooth, since only the envelopes of the heat flow rate, i.e., the maximum amplitudes, are used [10–12]. It is obvious that in this case rather long modulation periods are necessary to obtain correct heat capacity data. It was suggested that modulation periods of about 3–6 min reduce the error to about 2% for typical polymer samples. Without question,

steady state, alternating DSC (ADSC™) [10] is a powerful tool to separate thermal events of different kinetics, however, we believe that it might be useful and advantageous to apply the Fourier transformation also to such generated data sets, rather than using only the maximum amplitude to determine the heat capacity. Furthermore, we try to extract the correct heat capacity from one single data set, measured with a frequency ω_o, by analysis of the higher harmonics ν of the Fourier transform.

The Fourier analysis of the sample-temperature profile, $T_s(t)$, and heat flow rate response, $HF(t)$, for the determination of the heat capacity requires that the original data are not modified by anticipation of the temperature by the control procedure. Furthermore, it is common that the instrument software offers smoothing procedures to eliminate short term noise. Again depending on the smoothing procedure this may affect the output of the Fourier transform. Therefore, we will demonstrate and discuss, in addition to the experiments described above, how smoothing changes the overall profile of the heat flow rate $HF(t)$, and the afterwards performed Fourier transformation, needed for analysis with Eq. (4). A third common mathematical procedure which alters the originally gathered heat flow data is the subtraction of a baseline in the time-domain. We will continue earlier discussions to perform a correct asymmetry correction [13, 14], considering the specific calorimeter used in this study.

Experimental

The experiments were performed on a heat flux type calorimeter DSC 820 equipped with the ceramic sensor FRS5 (Mettler-Toledo GmbH). The instrument was operated with the liquid nitrogen accessory, and the furnace was purged with dry nitrogen at 80 ml min^{-1}. The temperature was calibrated using the melting temperatures of indium and zinc, extrapolated to zero heating rate (lag calibration), and the initial calibration of the heat flow rate was done using the heat of fusion of indium. Quasi-isothermal sawtooth-modulation in all experiments was performed at 299 K with a modulation amplitude of 1.0 K at different frequencies. Test samples used were sapphire (28.288 mg) and poly(ethylene-*co*-octene) (5.32–25.57 mg, 24 mass% 1-octene, 78.000 g mol^{-1}). These samples were selected because of their different thermal conductivities, and were used already in an earlier investigation using a power-compensating calorimeter (Perkin Elmer) [5, 7]. The copolymer sample was characterized in more detail with respect to the thermal behavior and its physical structure [15, 16]. The measurement of the apparent heat capacity under different experimental parameters, thermal history, and using DSC and TMDSC was used to verify truly reversible crystallization and melting [17]. Before analysis of the data, the baseline was subtracted as described later in this paper. If not stated otherwise, the 40 µl aluminum pans with a pin at the bottom were used for the experiments. The Fourier transformation of the sample temperature profile and heat-flow rate response was done with the instruments software (STAR^e V5.1), and the final calculation of the uncorrected, reversing heat capacity according to Eq. (4) with $K(\nu\omega)=1$.

Results and discussion

Frequency correction of the reversing heat capacity

Figure 1 is a plot of the uncorrected, specific heat capacity of sapphire (open symbols) and poly(ethylene-*co*-octene) (filled symbols) as a function of the modulation period. The measurements were performed at frequencies $2\pi/60$, $2\pi/120$ and $2\pi/240$ rad s^{-1}. The heat capacity was calculated using different harmonics of ν=1, 3, 5, 7, and 9, i.e., one single measurement produces data at five different frequencies.. All data of the three performed measurements fit a single function, which indicates that the higher harmonics behave exactly like the first harmonic, i.e., there is no non-linearity between sample temperature and heat flow response. The heat flow raw data are baseline-corrected in the time-domain using the same sample and reference pans as used for the baseline and sample runs. The dependence of the uncorrected specific heat capacity *vs*. the modulation period is similar, but more distinct to that which was measured earlier with a power-compensating calorimeter [5, 7]. In general, the uncorrected reversing heat capacity decreases with decreasing modulation period. The sapphire data begin to deviate from the theoretical value at a period of about 120 s, whereas the polymer sample starts to decrease already at about 200 s.

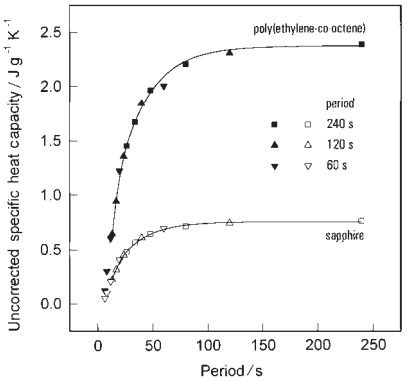

Fig. 1 Uncorrected specific heat capacity of sapphire (28.288 mg) and poly(ethylene-*co*-octene) (5.32 mg) as a function of the modulation period. The measurements were performed quasi-isothermally at 299 K with an amplitude of 1 K and periods of 60, 120 and 240 s. Heat capacities were calculated using Eq. (4) with $K(\nu\omega)$=1, and the first to ninth harmonic of the Fourier transform

Figures 2 and 3 are based on the data of Fig. 1 and show the inverse of the squared, uncorrected, specific heat capacities as a function of the square of the frequency in two magnifications. These plots visualize Eq. (6) and permit the evaluation of the corrected specific heat capacity and the time constant τ. Figure 2 extends to the modulation period p of 6.7 s (the ninth harmonic of a sawtooth of p=60 s), while Fig. 3 extends only to 13.3 s (the ninth harmonic of a sawtooth of p=120 s). In Fig. 2 a

clear non-linearity of the data can be recognized. It demonstrates that for larger frequencies τ becomes frequency-dependent. This, in turn, must be linked to the complex character of the heat transfer which cannot keep the temperature gradient within the sample at negligible levels. It is important to note, that we have measured the same behavior with the power-compensation calorimeter [5, 7], regardless of the fact that data in the latter instrument are shifted to a higher frequency. Closer inspection of the data in the low frequency range (Fig. 3), however, supports the validity of Eq. (6) in this limited frequency range. An extrapolation to zero frequency can now be done without difficulty. The intercept at $(\nu\omega)^2=0$ is the inverse of the squared, corrected, specific heat capacity, $(C_p^{corr})^{-2}$ and the slope is $(C_p^{corr})^{-2}\,\tau^2$. The linearity of the

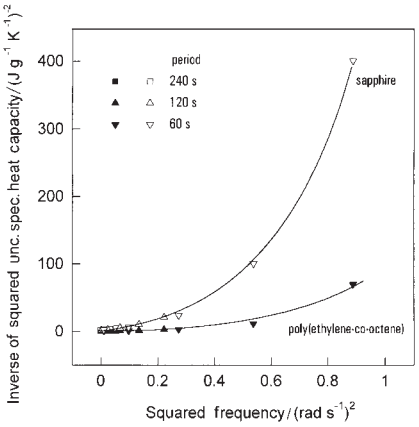

Fig. 2 Inverse of the squared, uncorrected, specific heat capacity as function of the square of the modulation frequency $\nu\omega$, using the data of Fig. 1

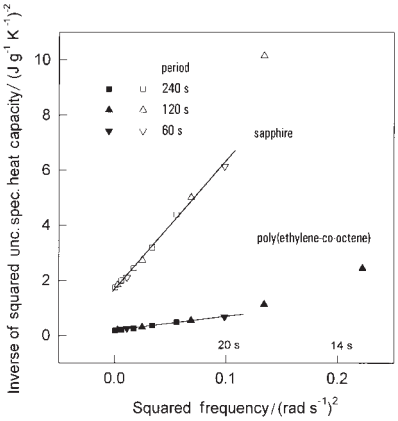

Fig. 3 Inverse of the squared, uncorrected, specific heat capacity as function of the square of the modulation frequency $\nu\omega$ in the low frequency range, using the data of Fig. 1

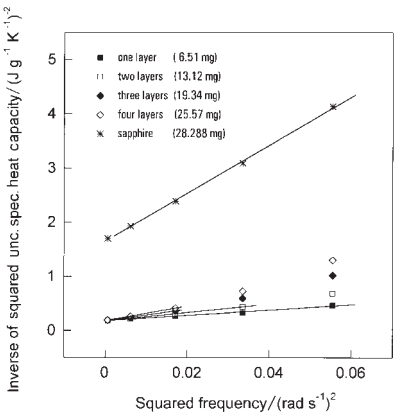

Fig. 4 Inverse of the squared, uncorrected, specific heat capacity as function of the square of the modulation frequency, obtained on poly(ethylene-*co*-octene)s with different sample thickness/mass during quasi-isothermal modulation at 299 K with an amplitude of 1 K. The modulation period is 240 s, and analysis was performed including data from the first to ninth harmonic of the Fourier transform

data is maintained to a squared frequency $(\nu\omega)^2$ of about 0.1 (rad s^{-1})^2 which corresponds to a modulation period of about 20 s (Fig. 3). The data are similar to that from our previous measurements using a power-compensation calorimeter, which maintain linearity to about 10–15 s modulation period, i.e., both instruments behave similar in this respect.

Figure 4 shows the inverse of the squared, uncorrected, specific heat capacity as a function of the square of the frequency, as in Figs 2 and 3, measured on poly(ethylene-*co*-octene) with different masses. The polymer sample was shaped into a film of thickness of about 200 μm. Measurements were performed on samples containing one (6.51 mg), two (13.12 mg), three (19.34 mg), and four (25.57 mg) layers of film. The modulation period was 240 s, and, as before, we analyzed data from the first to ninth harmonic of the Fourier transform of the heat flow rate and sample temperature. The experiment was done to explore the effect of sample thickness, mass, and perhaps the heat transfer conditions in the stack on our approach to extract the correct heat capacity. The increase of the sample thickness results in a change of the slope $(C_p^{corr})^{-2}\tau^2$ of the different data sets, whereas the extrapolated intercept remains constant. The change of the slope is caused by an increased time constant τ which is entirely due to τ_{sample} in Eq. (7), the instrument part of τ is unchanged since all other parameters of the experiment remained constant. Furthermore, we can see that the high-frequency limit of the linearity of the data sets in Fig. 4 is shifted to lower values when the sample mass in increased, as indicated by the drawn lines. Therefore, greatest care must be applied when selecting the squared frequency range for performing a linear fit to extract the intercept at $(\nu\omega)^2=0$. In fact, a nonlinear fit may be a better solution to obtain the correct heat capacity. In the case of using an arbitrary and more complicated function which contains more fitting parameters, it is straightforward to

apply the fitting procedure already to the original data [Eq. (4) with $K(\nu\omega)=1$] *vs*. the modulation period. However, we still would prefer to realize experimental conditions which guarantee the validity of Eq. (6) in a reasonable broad frequency range.

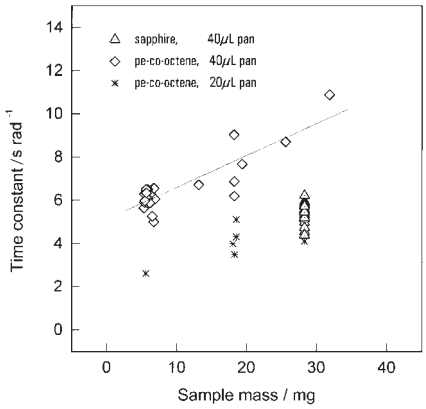

Fig. 5 Time constants τ of Eq. (6) as function of sample mass for poly(ethylene-*co*-octene) and sapphire. Additional data are included measured on poly(ethylene-*co*-octene) using the small 20 μl aluminum pan

An overview of time constants τ in s rad^{-1}, which were measured over several months on sapphire and poly(ethylene-*co*-octene) of different masses, is shown in Fig. 5. Additionally, in this plot are included measurements with the smaller aluminum pan of 20 μl (approximate mass 21 mg) instead of the standard 40 μl pan (approximate mass 48 mg). From Fig. 5 several conclusions can be drawn: (1) for a given sample mass, and restricting the pan size to 40 μl, the time constant is smaller for sapphire than for poly(ethylene-*co*-octene), (2) for a given sample mass, the time constant is smaller when using the 20 μl aluminum pan rather than the 40 μl aluminum pan, (3) the time constant increases approximately linearly with sample mass, and (4) repeated measurements reveal a statistical error of about 1 s rad^{-1}. All of these observations are as expected, lower thermal conductivity and higher absolute heat capacity give larger time constants. Extrapolation of the time constant of poly(ethylene-*co*-octene) to zero sample mass gives an instrumental time constant of approximately 5 s rad^{-1}, when using the larger, 40 μl aluminum pan, and about 2.5 s rad^{-1}, when using the lower mass, 20 μl aluminum pan. These values are reasonable when compared to the time constant of about 2 s rad^{-1} obtained with the power-compensation calorimeter (Perkin Elmer) with much smaller furnaces [5, 7].

Comments to the baseline correction

In the discussion of Figs 1 to 5, with respect to the accuracy and reproducibility of reversing heat capacities, we need to consider errors which might occur due to changes of the originally measured heat flow rate data prior the Fourier transformation. These

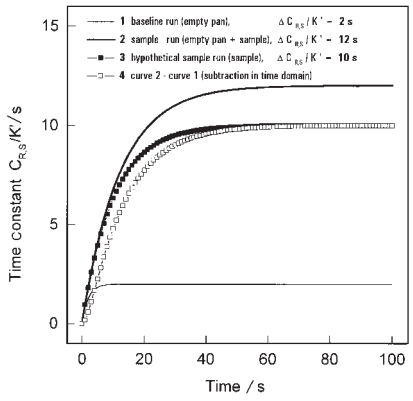

Fig. 6 Time constant $\Delta C_{R,S}/K'$ as function of time, calculated using Eq. (8) with values of $\Delta C_{R,S}/K'$ of 2, 10, and 12 s and an attempted baseline correction in the time domain

include (1) the subtraction of the baseline in the time domain, which is done only for the heat flow rate, and (2) smoothing of heat flow rate data to reduce the short term noise of the measurement. Baseline subtraction in the time-domain is common (and proper) practice in standard DSC to correct the amplitude of the heat flow rate for the asymmetry of the instrument [2]. The baseline is found by measuring the heat-flow rate with identical, empty sample and reference pans. In TMDSC, an additionally option for the asymmetry correction exists. One can calculate the apparent, reversing heat capacity with Eq. (4) from the run with empty, identical pans and extrapolation to frequency zero, as for the sample and calibration runs. Unfortunately the latter method is not able to assign the direction of the asymmetry because the phase information gets lost in the Fourier analysis. A suggested solution is the introduction of a known, additional asymmetry which pushes the heat flow rate to positive values [13]. The advantage of applying an amplitude-based baseline correction is the preservation of the direct correlation between sample temperature and heat flow rate before the Fourier transformation.

In case of subtracting the baseline in the time-domain, as frequently suggested [10, 18], an error results in the reversing apparent heat capacity, even though it is in most cases small, it can reach significance if the asymmetry becomes large [14]. The approach of steady state of the heat flow rate is given by [2]:

$$HF(t) \propto \Delta T = q \frac{\Delta C_{R,S}}{K'} \left(1 - e^{\frac{K'}{\Delta C_{R,S}} t} \right) \tag{8}$$

where ΔT is the measured temperature difference between reference and sample calorimeters, which is proportional to $HF(t)$, q is the heating rate, $\Delta C_{R,S}$ is the heat capacity difference between the sample and reference calorimeters, and K' is the appropriate Newton's law constant. In Fig. 6 the approach to steady state is shown for arbitrarily chosen values of $\Delta C_{R,S}/K'$=2 s (curve 1, thin line, simulating a baseline

run), $\Delta C_{R,S}/K'$=12 s (curve 2, heavy line, simulating a sample run of baseline + sample). The curve with $\Delta C_{R,S}/K'$=10 s (curve 3, filled squares) is the correct value for the sample only heat capacity (12 s–2 s=10 s). The calculated difference between the curves 2 and 1, which simulates the case of subtracting the heat flow rate in the time-domain, however, agrees only after steady state is reached (curve 4, open squares). The final amplitudes of curves 3 and 4 are identical, however, the approaches to steady state are different. In the standard DSC the heat capacity calculation would not be affected since only steady state data are used. In TMDSC the same is only possible when maintaining steady state in sinusoidal modulation. All sawtooth modulations, in contrast, include the approach to steady state within the Fourier transformation, and, therefore, the reversing heat capacity, calculated after baseline subtraction in the time domain, must contain an intrinsic error. However, we compared both type of analysis for the present measurements and equipment and found the differences insignificant within the reproducibility of about 1%. Nonetheless, at least when a precision of better than 1% is required, this error needs to be considered. The actual baseline correction is even more complicated since the heat flow rate profile is strongly distorted, probably, by the temperature control of the instrument. Each time, when changing the heating rate, a sharp spike appears in the heat flow rate as shown in Fig. 7. This spike is much larger in the baseline run, and makes it impossible to extract a corrected apparent baselineh eat capacity using Eqs (4) to (6).

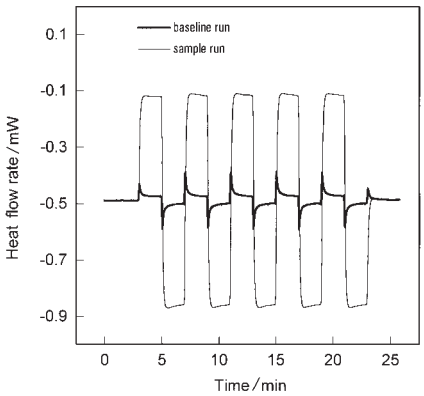

Fig. 7 The heat flow rate as function of time, for a baseline run consisting of empty pans (heavy line) and a sample run consisting of a sapphire sample + an empty pan (thin line)

Furthermore, the instrument's software permits an automatic baseline subtraction. If this option is used, the baseline heat flow rate is smoothed additionally to the standard-online-smoothing procedure which is described in the next section. The additional smoothing procedure removes the spike in the baseline run, however, subtraction of this curve results in a spike in the sample run instead. It must be concluded that this spike is also evident in the sample run, even if not visible due to the increased

amplitude, and it is not subtracted there anymore. Only if the not-smoothed baseline run is used for subtraction, does the corrected sample run show no spike at the switch from one rate to the next, because it is effectively subtracted. Figure 8 shows that the spikes are only effectively removed if not-smoothed data are used for the calculation.

Summarizing the discussion to the baseline correction in TMDSC, we believe that the accuracy in the determination of the reversing heat capacity is limited by the occurrence of discontinuities (spikes) at the switch from one rate of temperature change to the next. In the case of a linear, mass-independent superposition of this effect, a subtraction in the time-domain is the correct way to eliminate this artifact but this procedure violates the non-linear superposition of the two exponential functions which contain the baseline and sample heat capacities (Fig. 6). The latter error can simply be avoided when minimizing the asymmetry as much as possible, i.e., decrease the baseline amplitude to a maximum extent, and using relatively high sample mass. However, to high sample masses, in turn, are not recommended due to heat conduction problems, described in the discussion of Fig. 4.

Smoothing the heat flow rate

Smoothing is a widely used technique to reduce the short term noise of the heat flow raw data. The calorimeter used in this study performs an automatic online-smoothing during the measurement, which can, however, be defeated by the user. The change of the heat flow rate profile as result of smoothing affects the reversing heat capacity since the function given by Eq. (8) does not hold anymore, i.e., the heat flow response does not correspond anymore to the sample temperature change. Naturally, the smoothing will not affect the integrated heat flow, but will alter the various Fourier components, so that the corresponding Fourier component of the less or not smoothed sample temperature does not give the proper ratio in Eq. (4).

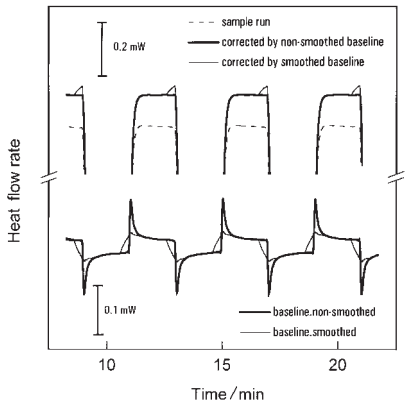

Fig. 8 The heat flow rate as function of time for a smoothed and non-smoothed baseline run (empty pan, bottom curves), a non-corrected sample run (sapphire + pan, dashed line of the upper curve), a smoothed baseline-corrected sample run (upper thin line), and a not-smoothed baseline corrected sample run (upper thick line)

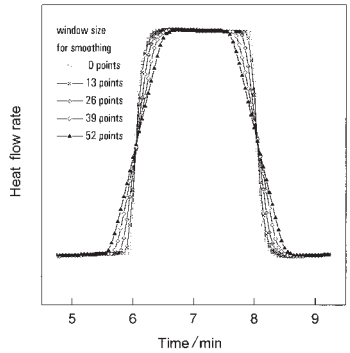

Fig. 9a The heat flow rate as function of time for a sample run (sapphire + pan), not-smoothed and smoothed using the window size given in the legend (zoomed for details)

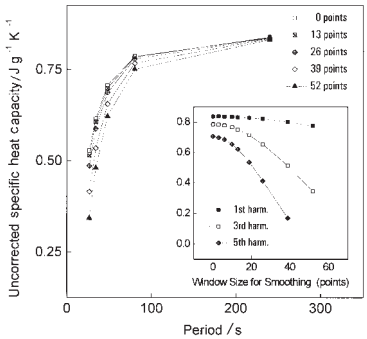

Fig. 9b Uncorrected specific heat capacity of sapphire as function of the modulation period, and the window size for smoothing (insert). Heat capacities are obtained using the data of Fig. 9a

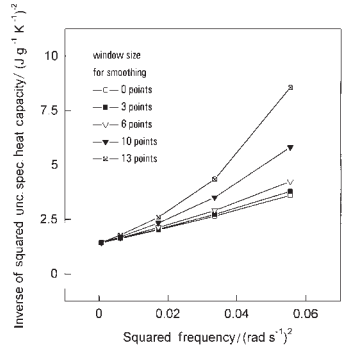

Fig. 9c Inverse of the squared, uncorrected specific heat capacity as function of the square of the modulation frequency, using the data shown in Figs 9a and b

Figure 9a shows the heat flow rate *vs*. time of a measurement on sapphire which was only smoothed automatically (on-line). Next, we continued the smoothing with different window sizes as given in the legend. Whereas the steady state amplitude is practically unchanged, the equilibration after switching from segment to the next is affected. Figure 9b illustrates the uncorrected specific heat capacity of sapphire as function of the modulation period, calculated using Eq. (4) with $K(\nu\omega)=1$, for different sized windows for smoothing. Figure 9c continues the analysis with a plot of the inverse of the squared uncorrected specific heat capacity as function of the square of the modulation frequency, using the data shown in Figs 9a and b. As expected, the almost rectangular heat flow rate profile of small τ is broadened (Fig. 9a), and the amplitude of the Fourier transform and, therefore, uncorrected reversing heat capacity for a given period and frequency is decreased (Fig. 9b). Again, the consequence of such a data treatment is the loss of the direct relationship between sample temperature and heat flow rate, resulting in an increasingly non-linear dependence between the inverse of the squared, uncorrected heat capacity *vs*. the square of the modulation frequency (Fig. 9c). Note it is still possible to extrapolate to the proper zero-frequency heat capacity, but not with the linear extrapolation. In fact, we cannot estimate the error due to smoothing of data, which is done on-line during the course of the measurement, if one does not have the not-smoothed raw data for comparison.

Conclusions

The heat flux calorimeter, used in this study, can advantageously be used for the quasi-isothermal determination of the reversing heat capacity based on a sawtooth-modulation of the program temperature and a Fourier transformation of the modulated heat flow rate and modulated heating rate. The heat capacity needs to be frequency-corrected by a calibration function, which takes into account the different equilibration behavior of the sample and reference calorimeters. When the calibration function is applied, heat capacities can be determined up to a frequency of about $(2\pi/20)$ rad s^{-1}. If no frequency calibration is performed, the heat capacity typically reaches the expected value at the much lower frequency of about $(2\pi/150)$ rad s^{-1}. The calibration can be done by using separate measurements at different frequencies, or, more effectively, by using the higher harmonics of one single measurement. An additional advantage when using the higher harmonics of one single measurement are the unchanged calorimeter configuration and sample properties and shape, which do affect the calibration function. The investigation has shown that many non-linear treatments of the measured heat flow rates, like baseline subtraction in the time domain and smoothing of the heat flow rate, distort the linearity between sample temperature and the heat flow response, and, in turn, affect the calculation of the reversing heat capacity.

Finally, based on these basic analyses, it became possible to apply a specialized sawtooth which was designed to have several harmonics of equal amplitude in its Fourier series [19] and obtain much higher precision than possible with a standard DSC when using the suggested method of nonlinear frequency extrapolation to zero

[20]. The same method has also being successfully applied to the TA Instrument MDSC™ [21] and the Perkin Elmer DDSC™ [22].

* * *

The author thanks Prof. B. Wunderlich for many helpful discussions concerning this study.

References

1 M. Reading, B. K. Hahn and B. S. Crowe, U.S. Patent, Method and Apparatus for Modulated Differential Analysis, 5, 224, 775, July 6, 1993; P. S. Gill, S. R. Sauerbrunn and M. Reading, J. Thermal Anal., 40 (1993) 931; M. Reading, A. Luget and R. Wilson, Thermochim. Acta, 138 (1994) 295.
2 B. Wunderlich, Thermal Analysis, Academic Press, New York 1990; for an update of the text see: Thermal Analysis of Materials, A computer-assisted lecture course published on the Internet (web.utk.edu/~athas/courses/tham99.html), downloadable including presentation software, 2000.
3 A. Boller, Y. Jin and B. Wunderlich, J. Thermal Anal., 42 (1994) 307.
4 B. Wunderlich, Y. Jin and A. Boller, Thermochim. Acta, 238 (1994) 277.
5 R. Androsch and B. Wunderlich, Thermochim. Acta, 333 (1999) 27.
6 B. Wunderlich and I. Okazaki, 'Temperature-Modulated Calorimetry of the Frequency Dependence of the Glass Transition of Poly(ethylene terephthalate) and Polystryrene' in M. R. Tant and A. J. Hills, eds., 'Structure and Properties of Glassy Polymers' ACS Symposium Series, 710 (1998) 103, Am. Chem. Soc., Washington, D.C.
7 R. Androsch, I. Moon, S. Kreitmeier and B. Wunderlich, Thermochim. Acta, in print.
8 J. E. K. Schawe and W. Winter, Thermochim. Acta, 298 (1997) 9.
9 I. Moon, R. Androsch and B. Wunderlich, Thermochim. Acta, accepted (1999); see also D. Dollimore (Ed.), Proceedings of the 26th NATAS Conference in Cleveland, OH, Sept. 13–15, 26 (1998) 134.
10 Manual Mettler-Toledo STAR^e Software Version 5.1.
11 R. Riesen, G. Wiedemann and R. Truttmann, Thermochim. Acta, 268 (1995) 1.
12 B. Schenker and F. Stäger, Thermochim. Acta, 304/305 (1997) 219.
13 K. Ishikiriyama and B. Wunderlich, J. Thermal Anal., 50 (1997) 337.
14 A. Boller, I. Okazaki, K.Ishikiriyama, G. Zhang and B. Wunderlich, J. Thermal Anal., 49 (1997) 1081.
15 R. Androsch, Polymer, 40 (1999) 2805.
16 R. Androsch, J. Blackwell, S. N. Chvalun and B. Wunderlich, Macromolecules, 32 (1999) 3735.
17 R. Androsch and B. Wunderlich, Macromolecules, 32 (1999) 7238.
18 Operating Instructions, Dynamic Differential Scanning Calorimetry (DDSC) Accessory Kit, Perkin Elmer, Norwalk, 1995.
19 B. Wunderlich, R. Androsch, M. Pyda and Y. K. Kwon, Thermochim. Acta, submitted September 1999.
20 J. Pak and B. Wunderlich, Thermochim. Acta, submitted October 1999.
21 M. Pyda, Y. K. Kwon and B. Wunderlich, Thermochim. Acta, submitted October 1999.
22 Y. K. Kwon, R. Androsch, M. Pyda and B. Wunderlich, Thermochim. Acta, submitted October 1999.